

Multifaceted Influences of Melanin-Like Particles on Amyloid-beta Aggregation

Haeun Song,^[a] Yoonyoung Kim,^[a] Inkyu Kim,^[a] Young-Kwan Kim,^[b] Sunbum Kwon,^[c] and Kyungtae Kang^{*[a]}

Abstract: The properties of eumelanin-like particles (EMPs) and pheomelanin-like particles (PMPs) in regulating the process of amyloid formation of amyloid-beta 42 (A β 42) were examined. EMPs and PMPs are effective both in interfering with amyloid aggregation of A β 42 and in remodeling matured A β 42 fibers. The results suggest that some (but not all) molecular species consisting of melanin-like particles (MPs) are responsible for their inhibiting property toward amyloid formation, and the influence is likely manifested by

long-range interactions. Incubating preformed A β 42 fibers with catechols or MPs leads to the formation of mesh-like, interconnected A β 42 fibers encapsulated with melanin-like material. MPs are kinetically more effective than catechol monomers in this process, and a detailed investigation reveals that 4,5-dihydroxyindole, a major intermediate in the formation of melanin-like species, and its derivatives are mainly responsible for remodeling amyloid fibers.

Introduction

Aberrant aggregation of proteins into amyloids—fibrillar aggregates rich in cross- β -sheet structures—has been connected to the pathologies of many fatal diseases. Soluble oligomeric species that form during aggregation or those equilibrating with insoluble fibers were shown to be cytotoxic, and thus have been considered central in the pathology of amyloid diseases.^[1–3] For decades, enormous efforts have been made to discover small molecules to inhibit the formation of amyloids or to remodel/disaggregate them. Polyphenols, among others, have received consistent interest, after the representative case of (–)-epigallocatechin gallate (EGCG), which was shown to inhibit and remodel the aggregation of pathological proteins (e.g. amyloid- β and α -synuclein).^[4–7] Many relevant studies using other polyphenols or catechols, such as baicalein,^[8–11] taxifolin,^[12] epicatechin,^[13] and brazillin^[14,15] for different amyloidogenic proteins/peptides showed similar results. In particular, the role of dopamine—one of the simplest biologically occurring catechols—in amyloid aggregation and the resultant pathology

of Parkinson's disease (PD) has been an important subject of studies,^[16,17] as PD occurs at a dopaminergic neuron-rich domain of a brain, the substantia nigra, and a significant amount of dopamine is found in Lewy bodies—the hallmark proteinaceous aggregates of PD.^[18,19] Yet natural polyphenols have been originally suspected, recent results collectively suggest that (i) catechol is the minimal molecular unit that can interfere with protein aggregation, (ii) its influences are general, with slightly different degrees, for many amyloidogenic proteins, and (iii) the O₂-driven auto-oxidation of catechols is somehow deeply involved in such influences. However, detailed molecular scale-explanations on how catechols perturb the aggregation kinetics of amyloidogenic species and its biochemical ramifications have not been made, due to the complicated natures of chemistries of amyloids and catechols.


In the presence of oxygen, dopamine self-oxidizes and undergoes several further transformations including cyclization and tautomerization,^[20] leading to the formation of poorly defined heterogeneous oligomeric mixtures often described as “melanin-like species”. This chemistry (or those relevant to it) has become especially useful for materials science, as such melanin-like species, at certain conditions, form thin films (“polydopamine” films) on any kind of surfaces in a material-independent manner.^[21,22] Quinone—a two electron-oxidized form of catechol-moieties embedded in polydopamine films can then be selectively cross-linked with biological nucleophiles (e.g., amines and thiols), which in turn enables substrate-independent covalent modification. Polydopamine shares many physicochemical properties (e.g., monotonic light absorption, photothermal properties, antioxidant ability, and permanent radical properties) with melanins, which have versatile roles in diverse biological contexts.^[23–26]

Emerging evidences collectively suggest the presence of perplexing, multifaceted interactions between amyloidogenic proteins (and their aggregation process) and catechols (and

[a] H. Song, Y. Kim, I. Kim, Prof. K. Kang
Department of Applied Chemistry
Kyung Hee University
1732 Deogyong-daero, Yongin, Gyeonggi 17104 (Republic of Korea)
E-mail: kkang@khu.ac.kr

[b] Prof. Y.-K. Kim
Department of Chemistry
Dongguk University
30 Pildong-ro 1-gil, Jung-gu, Seoul 04620 (Republic of Korea)

[c] Prof. S. Kwon
Department of Chemistry
Chung-Ang University
84 Heukseok-ro, Dongjak-gu, Seoul 06974 (Republic of Korea)

 Supporting information and the ORCID identification number(s) for the author(s) of this article can be found under:
<https://doi.org/10.1002/asia.201901405>.

their oxidative polymerization process). A few of hypotheses relying on the adduct formation between quinone groups of oxidized forms of catechols and amines or thiols of the protein residues have been proposed by mass spectrometric studies.^[12,27] In order to further investigate catechol-amyloid interactions, this work examines the properties of size-controlled melanin-like particles (MPs; eumelanin-like particles (EMPs) and pheomelanin-like particles (PMPs)) to perturb the aggregation process of amyloid-beta 42 (A β 42), and to remodel its pre-formed fibers. Metal^[28-31] or non-metal^[32-33] nanoparticles have been incorporated to perturb amyloid aggregation, but currently there is no report that used those of catechols. We intended to examine influences of MPs, as opposed to simple catechols, on amyloid aggregation with the following considerations: (i) quantitative kinetic analysis on amyloid formation relies mainly-if not exclusively-on Thioflavin T (ThT) fluorescence assay, which is an indirect measurement sensitive to the amount of β -sheet components. Catechols, however, possibly compete with ThT for binding to β -sheet structures, obscuring quantification of amyloid structures.^[34] (ii) We suspected that, if the reversible amine-quinone adduct formation mentioned above was the major contributor to the inhibitory effect, EMPs would bind to A β 42 and perturb its aggregation much stronger than catechols would, thanks to their multivalent nature. (iii) In such a case, the size of EMPs would be a critical factor, since the adduct formation is a surface-driven phenomenon, and varying the size of EMPs will also largely vary their surface area given the same mass concentration.

Results and Discussion

Size-controlled synthesis of MPs

Size-controlled EMPs were synthesized via a water-ethanol cosolvent method according to a previous work.^[35] PMPs were synthesized by simply adding cysteine to the synthetic procedure of EMPs to the desired ratio (Figure 1a).^[36] The synthesized MPs were analyzed by scanning electron microscopy (SEM), transmission electron microscopy (TEM) and X-ray photoelectron spectroscopy (XPS) for their size and atomic composition, respectively. The synthesized EMPs and PMPs had a spherical shape with a narrow range of diameters (Figure 1a). The size of particles could be controlled by varying the amount of ammonium hydroxide used in each synthesis (Figure 1b and Figure S1, S2). XPS analyses confirmed that EMPs and PMPs had the desired atomic compositions (Figure S3). Dynamic light scattering (DLS) analysis was conducted for MPs, and showed a similar trend in diameter with that determined by SEM images. Notably, EMPs and PMPs were similar in their surface zeta potential (Table 1).

Influences of the size of EMPs on their inhibitory ability to A β 42 aggregation

We initially sought to compare the inhibitory influences of EMPs with various diameters (135, 210, 315, and 450 nm) and catechol single molecules on the amyloid formation of A β 42.

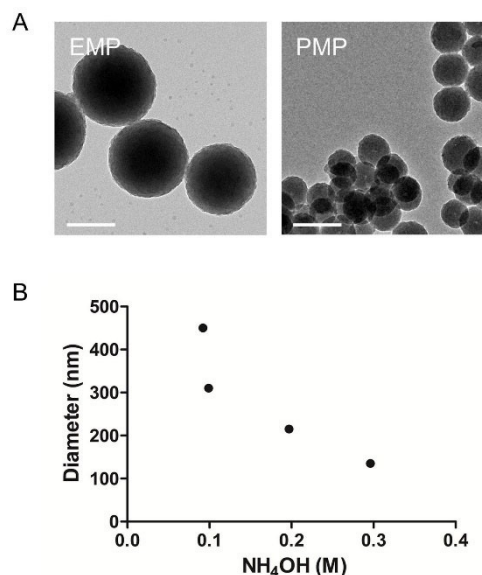


Figure 1. (a) TEM images of EMPs of a diameter of 315 nm (EMP₃₁₅; left) and PMP (right). The scale bars are 200 nm. (b) Diameters of EMPs synthesized with different concentrations of NH₄OH.

Table 1. Summary of physical properties of MPs.

	Diameter-SEM [nm]	Diameter-DLS [nm]	PDI	Zeta Potential [mV]
EMP ₁₃₅	134.57 ± 7.94	194.3	0.147	-25.3
EMP ₂₁₀	210.27 ± 9.85	290.4	0.120	-23.3
EMP ₃₁₅	314.43 ± 14.36	513.4	0.234	-33.7
EMP ₄₅₀	450.45 ± 12.98	572.1	0.269	-34.5
PMP	118.45 ± 9.79	165.4	0.062	-21.7

We first added catechols and their derivatives in the aggregation process of A β 42 (6.25 μ M). Since a molar concentration could not be readily used for EMPs, we used mass concentrations stoichiometrically equivalent to the molar concentrations of A β 42. Consistent with previous reports, dopamine and L-dopa (2.8 μ g mL⁻¹; 0.1-fold of the mass-equivalent of 6.25 μ M of A β 42) were very effective in decreasing the ThT fluorescence caused by amyloid aggregation (Figure 2a). The same amount of tyrosine had a marginal influence (less than 10% in intensity) on the fluorescence intensity, indicating that catechol moieties are central in interacting with the process of amyloid formation. The influence of dopamine was highly dose-dependent (Figure 2b); high concentrations (0.1-fold and 1-fold of A β 42, respectively) of dopamine led to both the reduction of ThT fluorescence intensity and a delay in aggregation kinetics, whereas lower concentrations had influences on ThT fluorescence but less so on the aggregation kinetics. It is well known that the initial concentration of amyloidogenic protein determines the lag time of the aggregation process.^[37] This result suggests that dopamine, when its concentration is high enough, is likely able to interact with monomeric A β 42 and inhibit its aggregation from the beginning, consistent with the previously reported amine- or thiol-quinone adduct formation.^[8,9,12]

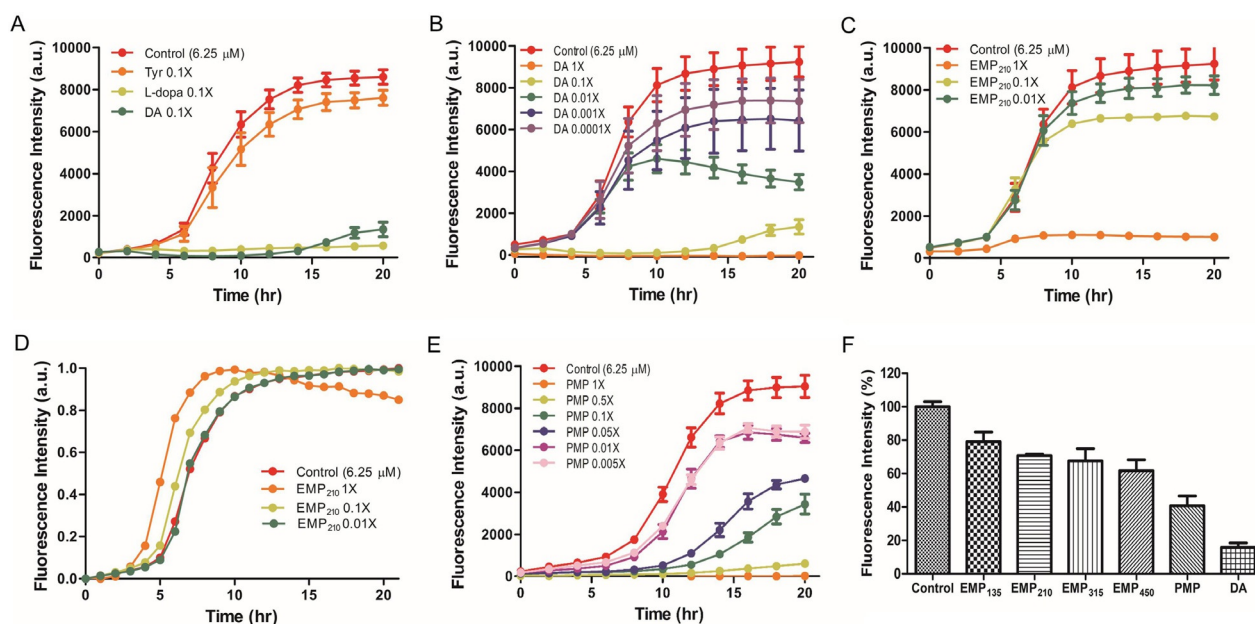


Figure 2. (a) ThT emission spectra with Aβ42 (6.25 μM) in the absence or presence of catechols (2.8 μg mL⁻¹; 0.1-fold of the mass-equivalent of Aβ42). (b-e) Dose-dependent inhibition of Aβ42 aggregation by (b) dopamine (DA), (c) EMP₂₁₀ and (e) PMP. (d) Normalized spectra of (c) in respect to the maximum value of each. (f) Normalized maximum ThT intensities ($F_{\max}-F_0$) in the presence of DA, EMPs and PMP (2.8 μg mL⁻¹; 0.1-fold of the mass-equivalent of 6.25 μM of Aβ42) in respect to the control sample.

Next, we examined the influences of EMPs on the aggregation of Aβ42. For the 0.1-fold conditions, we fit the fluorescence data to a sigmoidal curve to obtain kinetic parameters to describe the aggregation processes (Table S1). EMPs inhibited the Aβ42 aggregation, but with a less dose-efficiency than that of catechols (Figure 2c). Notably, altering the size of EMPs had less influence in their inhibiting properties, implying that the surface-driven interactions are not the major contributor in inhibiting amyloid formation (Figure S4). Also, addition of EMPs caused a dose-dependent decrease in ThT fluorescence intensity, but little change in the lag time of the aggregation process even at the high concentrations (Figure 2d). Taken together, the results indicate that EMPs likely interact with Aβ42 only after they form ThT-responsive (i.e., β-sheet-containing) species, and such interactions would be long-range (e.g., electron transfer), rather than direct surface binding. We also suggest that only a subset of EMP's constituents are active for interacting with amyloids, since dopamine monomers, which have potential to evolve to any component in the polydopamine-formation process, were much more effective than EMPs for preventing the formation of ThT-active species.

PMP regulates Aβ42 aggregation in a way different to how EMP does

Pheomelanin in nature, primarily rich in lips, nipples, and red hairs, is formed by a pathway similar to that of eumelanin,^[38] except the involvement of cysteine as an additional ingredient. Addition of cysteine results in reddish hue of the final material, and more importantly, largely different chemical properties, such as higher photosensitization tendency^[36,39] and more oxi-

dative redox potential, compared to eumelanin.^[40,41] We asked if PMPs would inhibit amyloid formation in a way similar to how EMPs do. PMPs were added to the aggregation pathway with the same concentrations used for EMPs. Alike EMPs, PMPs also showed a dose-dependent inhibition of Aβ42 aggregation. They, however, were more dose-effective than EMPs, indicating that PMPs contain more species reactive to amyloid. Notably, PMPs were more effective than EMPs both in decreasing fluorescence intensity and extending the lag time of Aβ42 aggregation (Figure 2e), suggesting that PMPs interact with Aβ42 in a different fashion to how EMPs do. Alike dopamine, PMPs seem to be capable of interacting with Aβ42 monomers effectively. Figure 2F compares the fitted values of maximum ThT intensities ($F_{\max}-F_0$) when dopamine and MP were added at the same concentration (0.1 X), showing that MP are generally less dose-efficient than dopamine, yet PMPs are more efficient than EMPs. Such a difference between EMPs and PMPs can be explained by their different redox properties; EMPs tend to give electrons, whereas PMPs prefer to receive electrons.^[42,43] This implies that electron transfer plays an important role in the interactions between MP and amyloid species.

Additions of EMPs and PMPs to Aβ42 result in different structures

To visually inspect the influences of MP and catechols on amyloid formation, we utilized TEM to directly observe species formed by aggregation of Aβ42 in the presence of MP and catechols. Aβ42 was incubated with catechols or MP for 24 h, and prepared for TEM analysis. In contrast to control samples and those treated with tyrosine (Figure 3a and 3b), Aβ42 incu-

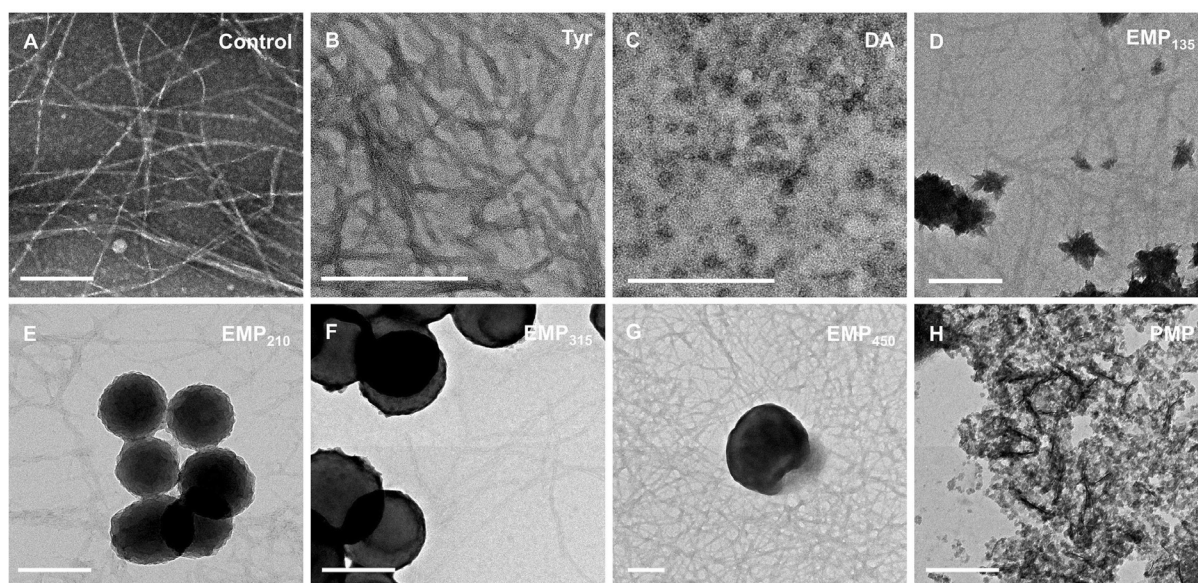


Figure 3. TEM images of A β 42 (6.25 μ m; 37 $^{\circ}$ C, 10 mM PBS 7.4) incubated for 24 h in the absence (a) or presence of tyrosine (b), dopamine (c), EMPs (d–g), and PMPs (h). The scale bars are 200 nm.

bated with *L*-dopa and dopamine (28 μ g mL $^{-1}$; 1-fold of the mass-equivalent of 6.25 μ m of A β 42) showed amorphous aggregates without fibrillary structures (Figure 3 c). However, incubation with various sizes of EMPs (1X) led to the formation of a few, but clear fibrillary structures (Figure 3 d–g). This was unexpected, considering that we observed almost no ThT signals at these conditions. Compared to the thickness of bare A β 42 fibers (Figure 3 a; 9.36 ± 1.27 nm), those formed with EMPs were slightly thicker (Figure S5; 12.60 ± 1.75 , 11.21 ± 1.68 , 10.40 ± 1.87 , and 12.63 ± 1.95 nm for EMPs with diameters of 135, 210, 315, and 450 nm, respectively). EMPs were primarily observed as intact morphologies, but in some cases they were partially dissolved within fiber structures nearby, forming poly-dopamine-fiber composites (Figure 3 d and 3 g). These results suggested the possibility that the fibers were coated with molecular species that came out of EMPs. When incubated with PMPs, there were neither intact PMP structures nor A β 42 fibers. Instead, PMPs were completely fragmented and formed amorphous, mesh-like structures with A β 42, as the case of catechol monomers (Figure 3 h). These results explain the above results of ThT assay: EMPs react with preformed amyloid species, whereas PMPs can react with the monomeric state. This is in line with previous reports in which pheomelanin-like species were shown to behave self-destructively when undergoing redox reactions.^[44] TEM analyses further supported that EMPs and PMPs interact with A β 42 and modulate its aggregation by chemically different mechanisms.^[45]

MPs and 5,6-dihydroxyindole (DHI) remodel matured A β 42 fibers faster than catechols do

Catechols or polyphenols that inhibit the aggregation process of amyloidogenic proteins are often also active in remodeling (or disassembling) preformed amyloid fibers. Kelly et al. specifi-

cally focused on such a property of EGCG toward various forms of amyloids, and suggested that hydrophobic interactions between surface of amyloids and EGCG would be the major driving factor.^[46] Despite a quite large amount of efforts, it is still unclear how catechols interact with matured amyloid fibers in respect to the following points: (i) Is there a general mechanism that can explain all the interactions between catechol-containing molecules and amyloids of different proteins? (ii) Do catechols indeed disassemble cross β -sheet structures in amyloids, or just make them invisible to ThT fluorescence? (iii) Is there a single mechanism that underlies both catechol-based inhibition of amyloid aggregation and catechol-based remodeling of amyloid fibers? To examine the interactions between catechols/MPs and matured amyloid fibers, we first generated matured amyloid fibers of A β 42, and incubated them with an excess amount of ThT for 8 h to saturate the binding sites of ThT on fibers. ThT-saturated fibrils were centrifuged at 15000 rpm for 10 min for removing unbound ThT. The fibers (6.25 μ m) were then treated with catechols (1-fold of 6.25 μ m of A β 42-equivalent) and MPs (1-fold of 6.25 μ m of A β 42-equivalent). As shown in Figure 4 a and 4 b, catechols (dopamine, *L*-dopa, and epinephrine) and MPs of various sizes decreased the ThT fluorescence of the A β 42 fibers gradually. Tyrosine was not effective, indicating that catechol moieties are, again, crucial in fiber-remodeling properties. Here, all the catechol-treated samples showed an initial bump (2–5 h, approximately) where the fluorescence intensity did not decrease significantly, whereas treating MPs caused an immediate decrease of ThT fluorescence upon addition (Figure 4 b). Differences between EMPs and PMPs were not noticeable. These results imply that catechols are initially inactive to fibers, and they have to react each other to generate molecular species capable of disrupting ThT binding to fibers. MPs, on the other hand, seem to already contain such species, which are likely one of the components

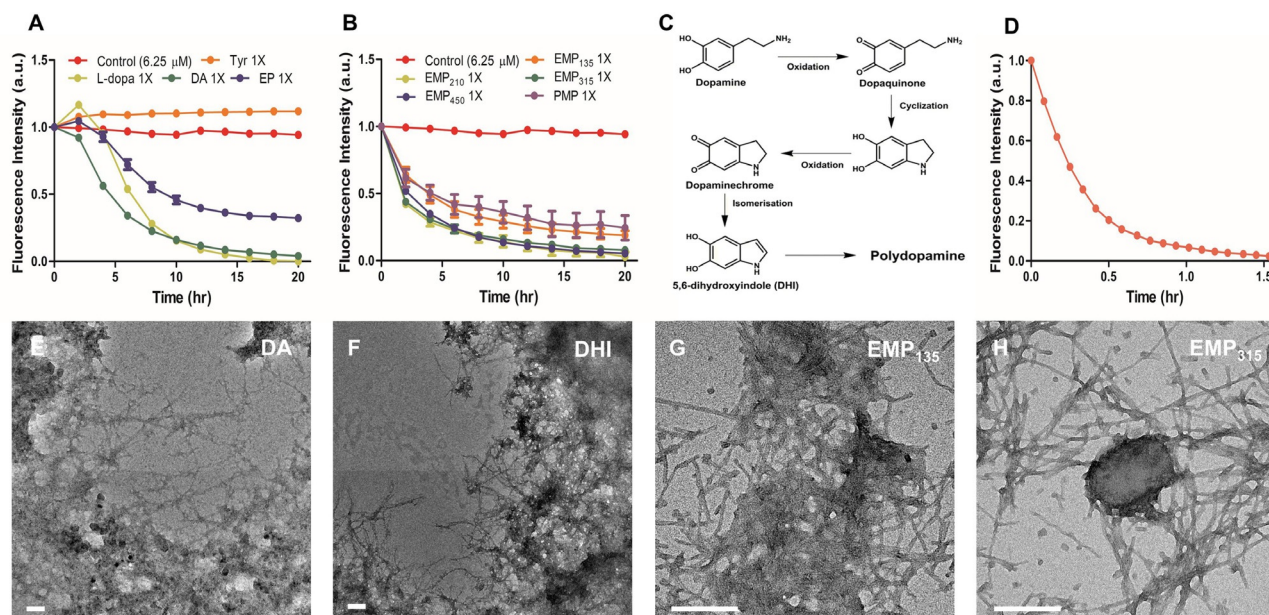


Figure 4. Normalized ThT emission spectra of ThT-saturated A β 42 fibers treated with (a) catechols or (b) MPs ($28 \mu\text{g mL}^{-1}$; 1-fold of the mass-equivalent of $6.25 \mu\text{M}$ of A β 42). (c) Schematic illustration of polydopamine formation. (d) Normalized ThT emission spectra of ThT-saturated A β 42 fibers treated with DHI ($28 \mu\text{g mL}^{-1}$; 1-fold of the mass-equivalent of $6.25 \mu\text{M}$ of A β 42). (e–h) TEM images of matured A β 42 fibers incubated for 24 h in the presence of (e) dopamine, (f) DHI, (g) EMP₁₃₅, and (h) EMP₃₁₅. All samples were incubated at 37°C , and the scale bars are 200 nm.

of polydopamine species, or intermediates during its synthesis. To this end, we chemically synthesized DHI, which is known to be one of the major intermediates in polydopamine (and eumelanin) formation (Figure 4c), and asked if it differs from catechols in interacting with amyloid fibers. Addition of DHI (1-fold of $6.25 \mu\text{M}$ of A β 42-equivalent) caused an extremely fast decrease in ThT signal, which was even faster than the cases of MPs (Figure 4d). O₂-driven auto-oxidation of dopamine leads to the formation of DHI, which is then self-polymerized and complexed to form polydopamine (or, melanin-like species). Based on this, we could speculate that DHI or its small oligomers are primarily responsible for interacting with A β 42 species. This explains the different inhibition efficiencies between dopamine and EMPs, as EMPs contain a small portion of DHI and its oligomers, whereas dopamine would eventually turn to DHI, which are captured by A β 42 species, driving the proportionation equilibrium toward DHI. When incubated with soluble A β 42, DHI inhibited the formation of amyloid fibers in a dose-dependent manner, remarkably without a delay in the lag time (Figure S7). This result implies that DHI primarily interact with β -sheet-containing species, as the case of MPs.

When observed via TEM, A β 42 fibers incubated with catechols or DHI showed mesh-like structures (Figure 4e and 4f). However, the structures were different from the amorphous aggregates shown in Figure 3, as they were composed of clear fibrillary structures densely coated with dark melanin-like species, by which the fibers were interconnected. Fibers incubated with EMPs also showed similar mesh-like structures (Figure 4g and 4h). In this case, EMPs were partially disintegrated and permeated to the surrounding A β 42 fibers. These results suggest that, for both cases (incubating with catechols and MPs), DHI-based melanin-like species were formed preferentially near

the fibers, resulting in ThT-invisible fiber-melanin composites. This is reminiscent of the process of melanin biosynthesis, where a kind of amyloid fibers composed of an intramelanosomal protein-Pmel17-is involved as a catalytic scaffold. Amyloid fiber matrix of Pmel17 is known to recruit and sequester potentially harmful intermediates of melanin by an unclear molecular mechanism.^[47,48] Our results imply that there is an intrinsic favorable interaction between DHI species and amyloid structures, which is simultaneously responsible for the regulatory role of Pmel17 amyloids in melanin biosynthesis and the frequently seen modulation of amyloid species by catechols.

Conclusions

In this work, we examined the influences of catechols and MPs on the process of amyloid formation and their capability of remodeling matured amyloids. The results show that (i) MPs partially contain molecular species that can interfere with amyloid species (but not the monomeric state) likely by non-surface-driven interactions. (ii) PMPs differ largely from EMPs in their interactions with A β 42, and perturb A β 42 aggregation from its monomeric state. (iii) Adding MPs or catechols to matured A β 42 fibers does not disassemble them, but rather leads to the formation of mesh-like structures composed of the fibers encapsulated by melanin-like species, invisible by ThT. (iv) MPs are more effective than catechol monomers in such influences, likely because DHI-related intermediates in polydopamine formation are the major species reactive to A β 42 fibers. Thanks to their biocompatibility (Figure S8 shows MPs are also biocompatible) and accessibility, using catechols or polyphenols as a candidate to suppress amyloid species and their pathological influences has received great interests. This idea, however,

would become feasible only with understanding the molecular mechanism by which catechols interact with the characteristic supramolecular structure of amyloids—considering that amyloids made of various proteins have interactions with catechols in common, it is likely that the amyloid structure (rather than a single domain/sidechain/functional group) is reactive to catechol species. Results of the current work and others clearly indicate that catechols have inherently multifaceted and complicated interactions with amyloids, which would obscure their applications mentioned above. In addition, the linkage between extracellular amyloid species and the onset of neurodegenerative diseases is being frequently doubted.

Nonetheless, the findings of this work suggest that amyloid-catechol interactions merit further interests from the field of chemistry. Amyloid-catechol interactions appear in melanin biosynthesis, where functional amyloid fibers made of Pmel17 are active in facilitating melanin biosynthesis, sequestering toxic intermediates, and other functions.^[37] Influences of catechols on amyloid aggregation or remodeling may be one aspect of amyloid-catechol interactions, leaving more potentially important and chemically interesting areas unexplored. In particular, chemical functionality—toward catechols, in this case—that arises by the supramolecular structure of amyloid fibers can be the key to understand the chemistries of functional amyloids and the chemical origins of amyloid-based cytotoxicity.

Experimental Section

Materials

Dopamine hydrochloride, *L*-cysteine, tyrosine, (–)-epinephrine, ThT, and potassium permanganate (KMnO₄) were purchased from Sigma–Aldrich. 3,4-Dihydroxy-*L*-phenylalanine (*L*-dopa) and phosphotungstic acid hydrate were purchased from Alfa-Aesar. Aβ42 was purchased from Anaspec.

Synthesis of MP

EMPs were prepared using a 1:2 water-ethanol co-solvent system. A desired amount of aqueous ammonia solution (28 to 30%) was added to 130 mL of the solvent, and the mixture was stirred gently for 30 min. 0.5 g of dopamine-hydrochloric acid was dissolved completely in 10 mL of distilled water, and then added to the mixed solution. The solution was initially yellowish brown and turned black gradually. After incubating for 24 h at room temperature under vigorous stirring, EMPs were rinsed with distilled water and spun down at 15000 rpm. PMPs were synthesized by using water as a solvent. 70 mg of *L*-dopa was completely dissolved in 50 mL of distilled water under heating, followed by addition of 85.6 mg of *L*-cysteine and 360 μL of 1 N KMnO₄. The reaction was proceeded for 24 h under vigorous stirring. The products were then spun down at 15000 rpm and redispersed in 50 mL distilled water. 1 N hydrochloric acid was added slowly to sequester Mn²⁺ in the solution, and then the products were rinsed with distilled water three times with centrifugation. The synthesized MPs were lyophilized and stored at room temperature until usage. The SEM images were acquired on a Hitachi S-4800 FESEM with a cover glass. The hydrodynamic diameter of particles and zeta potentials were measured by DLS using a Malvern Nano ZS ZEN3690 instru-

ment. Measurements were averaged over 18 runs in deionized water.

Analyses of Aβ42 aggregation and remodeling of fibers

Aβ42 was first dissolved in an aqueous solution of ammonium hydroxide (NH₄OH, 1% v/v), aliquoted, and lyophilized for storage at –80 °C. The lyophilized peptide was dissolved in 10 μL of 1% NH₄OH and diluted with water to prepare a stock solution (≈100 μM). The peptide stock solution was then diluted in phosphate buffered saline (pH 7.4) to desired concentrations by measuring absorbance at 280 nm using Eppendorf BioPhotometer D30 (extinction coefficient: 1490 cm⁻¹·M⁻¹). For visualizing amyloid species, ThT was diluted to a final concentration of 6.25 μM. When the aggregation was complete, the solution containing fibers was centrifuged at 12000 rpm to remove unaggregated Aβ42. Here, the concentrations of unaggregated Aβ42 remaining in the supernatant was measured by using the spectrophotometer, which gave the concentration of Aβ42 fibers as well. The measured concentrations were cross-checked by using the bicinchoninic acid assay (BCA assay). MPs or catechol monomers were added to solutions of Aβ42 and then ThT fluorescence (450 nm excitation, 490 nm emission) was measured while incubating for 24 h at 37 °C. For the fiber-remodeling experiments, MPs or catechol monomers were added to solutions of matured Aβ42 fibers, which were synthesized by agitation at 200 rpm for 24 h at 37 °C.

Synthesis of DHI

The methods is similar to those reported.^[49] An aqueous solution (400 mL) of 3,4-dihydroxy-*L*-phenylalanine (98+%; 804.9 mg (4 mmol)) and an aqueous solution (48 mL) of potassium ferricyanide (5.268 g, 16 mmol) and sodium bicarbonate (2.0162 g, 24 mmol) were separately degassed by purging with N₂ flux for 10 min. The two solutions were then mixed and stirred at room temperature. After 2 h, when the reddish color of the solution disappeared, sodium metabisulfite (3.9543 g, 20.8 mmol) was added. The resulting solution was extracted with ethyl acetate (three times with 240 mL). The combined extracts were washed once with brine (80 mL), and dried over anhydrous sodium sulfate. The solvent was removed by rotatory evaporator, and residual brown oil was dissolved in acetone (2.4 mL) and benzene (24 mL) first, and then hexane (16 mL) was added. The black melanin precipitate was removed by filtration and the resulting brown solution was gradually mixed with hexane (100 mL) to get colorless DHI crystals. The mixture was kept overnight at 4 °C and the crystals were filtered and dried to give the final product (40% yield).

TEM analysis

FCF200-CU grid were treated with samples (10 μL, 6.25 μM Aβ42) for 2 min at room temperature. Excess sample was washed with distilled water. The grid was stained with phosphotungstic acid hydrate (1% w/v, distilled water, 5 μL, for 1 min), then washed and dried for 5 min at 60 °C in a dry-oven. TEM images were taken by using JEM-2100F (JEOL) transmission electron microscope (200 kV).

Cell culture

Human neuroblastoma SH-SY5Y were obtained from Korean Cell Line Bank (Seoul, Korea), grown in MEM medium supplemented with 10% fetal bovine serum, 1% antibiotics at 37 °C and 5% CO₂.

Cytotoxicity assay

Cells were plated in 96-well plates at a density of 40000 cells per well containing growth medium, and cultured for 24 h. For the assay, the cells were incubated with a desired concentration ($28 \mu\text{g mL}^{-1}$) of MPs in 200 μL of medium supplemented with 3% fetal bovine serum for 24 h at 37 °C. After the treatment, medium was removed and the cells were wash with DPBS for three times. cell viability was measured by WST-1 assay. Briefly, 10 μL of the WST-1 solution was added to each well with 100 μL of fresh medium and incubated for 1 h at 37 °C. The absorbance was measured at 450 nm with a microplate reader.

Acknowledgements

This work was supported by the National Research Foundation of Korea (NRF) grant funded by the Ministry of Science, ICT&Future Planning (MSIP) (2019R1C1C1009111), the GRRC program of Gyeonggi province [GRRC-kyunghee2017(A01)], and a grant from Kyung Hee University in 2016 (KHU-20160610).

Conflict of interest

The authors declare no conflict of interest.

Keywords: amyloid beta-peptides • amyloids • bioorganic chemistry • melanin-like particles • polydopamine

- [1] C. Haass, D. J. Selkoe, *Nat. Rev. Mol. Cell Biol.* **2007**, *8*, 101–112.
- [2] R. Kaye, E. Head, J. L. Thompson, T. M. McIntire, S. C. Milton, C. W. Cotman, C. G. Glabe, *Science* **2003**, *300*, 486–489.
- [3] S. J. C. Lee, E. Nam, H. J. Lee, M. G. Savelieff, M. H. Lim, *Chem. Soc. Rev.* **2017**, *46*, 310–323.
- [4] J. Bieschke, J. Russ, R. P. Friedrich, D. E. Ehrnhoefer, H. Wobst, K. Neugebauer, E. E. Wanker, *Proc. Natl. Acad. Sci. USA* **2010**, *107*, 7710–7715.
- [5] J. M. Lopez del Amo, U. Fink, M. Dasari, G. Grelle, E. E. Wanker, J. Bieschke, B. Reif, *J. Mol. Biol.* **2012**, *421*, 517–524.
- [6] S.-J. Hyung, A. S. DeToma, J. R. Brender, S. Lee, S. Vivekanandan, A. Kochi, J.-S. Choi, A. Ramamoorthy, B. T. Ruotolo, M. H. Lim, *Proc. Natl. Acad. Sci. USA* **2013**, *110*, 3743–3748.
- [7] J. E. Yang, K. Y. Rhoo, S. Lee, J. T. Lee, J. H. Park, G. Bhak, S. R. Paik, *Sci. Rep.* **2017**, *7*, 17945.
- [8] P. Velander, L. Wu, W. K. Ray, R. F. Helm, B. Xu, *Biochemistry* **2016**, *55*, 4255–4258.
- [9] M. Zhu, S. Rajamani, J. Kaylor, S. Han, F. Zhou, A. L. Fink, *J. Biol. Chem.* **2004**, *279*, 26846–26857.
- [10] D.-P. Hong, A. L. Fink, V. N. Uversky, *J. Mol. Biol.* **2008**, *383*, 214–223.
- [11] X. Meng, L. A. Munishkina, A. L. Fink, V. N. Uversky, *Biochemistry* **2009**, *48*, 8206–8224.
- [12] M. Sato, K. Murakami, M. Uno, Y. Nakagawa, S. Katayama, K.-i. Akagi, Y. Masuda, K. Takegoshi, K. Irie, *J. Biol. Chem.* **2013**, *288*, 23212–23224.
- [13] R. C. George, J. Lew, D. J. Graves, *J. Alzheimer's Dis.* **2013**, *36*, 21–40.
- [14] W.-J. Du, J.-J. Guo, M.-T. Gao, S.-Q. Hu, X.-Y. Dong, Y.-F. Han, F.-F. Liu, S. Jiang, Y. Sun, *Sci. Rep.* **2015**, *5*, 7992.
- [15] J. Guo, W. Sun, L. Li, F. Liu, W. Lu, *RSC Adv.* **2017**, *7*, 43491–43501.
- [16] D. E. Mor, E. Tsika, J. R. Mazzulli, N. S. Gould, H. Kim, M. J. Daniels, S. Doshi, P. Gupta, J. L. Grossman, V. X. Tan, *Nat. Neurosci.* **2017**, *20*, 1560–1568.
- [17] J. Xu, S.-Y. Kao, F. J. Lee, W. Song, L.-W. Jin, B. A. Yankner, *Nat. Med.* **2002**, *8*, 600–606.
- [18] M. Baba, S. Nakajo, P.-H. Tu, T. Tomita, K. Nakaya, V. Lee, J. Q. Trojanowski, T. Iwatsubo, *Am. J. Pathol.* **1998**, *152*, 879–884.
- [19] W. Gibb, A. Lees, *J. Neurol. Neurosurg. Psychiatry* **1988**, *51*, 745–752.
- [20] Y. Liu, K. Ai, L. Lu, *Chem. Rev.* **2014**, *114*, 5057–5115.
- [21] H. Lee, S. M. Dellatore, W. M. Miller, P. B. Messersmith, *Science* **2007**, *318*, 426–430.
- [22] B. P. Lee, P. B. Messersmith, J. N. Israelachvili, J. H. Waite, *Annu. Rev. Mater. Res.* **2011**, *41*, 99–132.
- [23] B. H. Kim, D. H. Lee, J. Y. Kim, D. O. Shin, H. Y. Jeong, S. Hong, J. M. Yun, C. M. Koo, H. Lee, S. O. Kim, *Adv. Mater.* **2011**, *23*, 5618–5622.
- [24] J. H. Ryu, P. B. Messersmith, H. Lee, *ACS Appl. Mater. Interfaces* **2018**, *10*, 7523–7540.
- [25] W. Sheng, B. Li, X. Wang, B. Dai, B. Yu, X. Jia, F. Zhou, *Chem. Sci.* **2015**, *6*, 2068–2073.
- [26] I. You, Y. C. Seo, H. Lee, *RSC Adv.* **2014**, *4*, 10330–10333.
- [27] S. Jongberg, S. N. E. Gislason, M. N. Lund, L. H. Skibsted, A. L. Waterhouse, *J. Agric. Food Chem.* **2011**, *59*, 6900–6905.
- [28] N. Xiong, Y. Zhao, X. Dong, J. Zheng, Y. Sun, *Small* **2017**, *13*, 1601666.
- [29] H.-M. Chan, L. Xiao, K.-M. Yeung, S.-L. Ho, D. Zhao, W.-H. Chan, H.-W. Li, *Biomaterials* **2012**, *33*, 4443–4450.
- [30] Y. D. Álvarez, J. A. Fauerbach, J. s. V. Pellegrotti, T. M. Jovin, E. A. Jares-Erijman, F. D. Stefani, *Nano Lett.* **2013**, *13*, 6156–6163.
- [31] A. Gladysz, B. Abel, H. J. Risselada, *Angew. Chem. Int. Ed.* **2016**, *55*, 11242–11246; *Angew. Chem.* **2016**, *128*, 11408–11412.
- [32] K. Debnath, N. Pradhan, B. K. Singh, N. R. Jana, N. R. Jana, *ACS Appl. Mater. Interfaces* **2017**, *9*, 24126–24139.
- [33] Y. Li, Z. Du, X. Liu, M. Ma, D. Yu, Y. Lu, J. Ren, X. Qu, *Small* **2019**, *15*, 1901116.
- [34] S. A. Hudson, H. Ecroyd, T. W. Kee, J. A. Carver, *FEBS J.* **2009**, *276*, 5960–5972.
- [35] K. Ai, Y. Liu, C. Ruan, L. Lu, G. Lu, *Adv. Mater.* **2013**, *25*, 998–1003.
- [36] J. Pyo, K.-Y. Ju, J.-K. Lee, *J. Photochem. Photobiol. B* **2016**, *160*, 330–335.
- [37] W.-F. Xue, S. W. Homans, S. E. Radford, *Proc. Natl. Acad. Sci. USA* **2008**, *105*, 8926–8931.
- [38] R. Micillo, L. Panzella, K. Koike, G. Monfrecola, A. Napolitano, M. d'Ischia, *Int. J. Mol. Sci.* **2016**, *17*, 746.
- [39] T. Sarna, I. Menon, R. C. Sealy, *Photochem. Photobiol.* **1985**, *42*, 529–532.
- [40] E. Kim, L. Panzella, L. R. Micillo, W. E. Bentley, A. Napolitano, G. F. Payne, *Sci. Rep.* **2015**, *5*, 18447.
- [41] A. Samokhvalov, L. Hong, Y. Liu, J. Garguilo, R. J. Nemanich, G. S. Edwards, J. D. Simon, *Photochem. Photobiol.* **2005**, *81*, 145–148.
- [42] M. d'Ischia, K. Wakamatsu, A. Napolitano, S. Briganti, J. C. Garcia-Borron, D. Kovacs, P. Meredith, A. Pezzella, M. Picardo, T. Sarna, *Pigment Cell Melanoma Res.* **2013**, *26*, 616–633.
- [43] A. Napolitano, L. Panzella, G. Monfrecola, M. d'Ischia, *Pigment Cell Melanoma Res.* **2014**, *27*, 721–733.
- [44] M. R. Chedekel, S. K. Smith, P. W. Post, A. Pokora, D. L. Vessell, *Proc. Natl. Acad. Sci. USA* **1978**, *75*, 5395–5399.
- [45] S. Ito, K. Wakamatsu, T. Sarna, *Photochem. Photobiol.* **2018**, *94*, 409–420.
- [46] F. L. Palhano, J. Lee, N. P. Grimster, J. W. Kelly, *J. Am. Chem. Soc.* **2013**, *135*, 7503–7510.
- [47] D. M. Fowler, A. V. Koulov, C. Alory-Jost, M. S. Marks, W. E. Balch, J. W. Kelly, *PLOS Biol.* **2005**, *4*, e6.
- [48] R. P. McGlinchey, T. L. Yap, J. C. Lee, *Phys. Chem. Chem. Phys.* **2011**, *13*, 20066–20075.
- [49] L. Panzella, G. Gentile, G. D'Errico, N. F. Della Vecchia, M. E. Errico, A. Napolitano, C. Carfagna, M. d'Ischia, *Angew. Chem. Int. Ed.* **2013**, *52*, 12684–12687; *Angew. Chem.* **2013**, *125*, 12916–12919.

Manuscript received: October 8, 2019

Revised manuscript received: November 6, 2019

Version of record online: November 28, 2019